

Specific three-loop contributions to $b \rightarrow s\gamma$ associated with the current-current operators

Christoph Greub^a, Hrachia M. Asatryan^b, Francesco Saturnino^a and Christoph Wiegand^a

^a*Albert Einstein Center for Fundamental Physics, Institute for Theoretical Physics,
University of Bern, CH-3012 Bern, Switzerland*

^b*Yerevan Physics Institute, 0036 Yerevan, Armenia*

Abstract

We work out a specific class of three-loop diagrams (of order α_s^2) contributing to the decay amplitude for $b \rightarrow s\gamma$ associated with the current-current operators O_1 and O_2 at the physical value of the charm-quark mass m_c . For many of the considered diagrams we were able to solve the master integrals using differential equations in the canonical form. For some diagrams we did not find a transformation to canonical form and therefore calculated the corresponding master integral directly as an expansion around $z = m_c^2/m_b^2 = 0$, retaining power terms up to z^{10} and keeping the accompanying $\log(z)$ terms to all powers. The results for the sum of all considered diagrams are given in tabular form, while contributions of individual diagrams (or combinations thereof) are given in electronic form.

Contents

1	Introduction	2
2	Theoretical framework	3
3	Reduction of the decay amplitude to Master Integrals	3
3.1	Form factor decomposition and scalar integrals	5
3.2	IBP reduction and Master integrals	6
3.3	Differential equations for the Master integrals	7
3.4	Methods used to calculate the Master Integrals	7
4	Solving MIs via canonical form	7
4.1	Canonical form and iterative solution	8
4.2	Fixing integration constants	9
4.3	Expansion around $z = 0$	11
5	Calculating the MIs in sets (11, 12) and (13, 14)	11
5.1	Solving the differential equations as an expansion for small z	11
5.2	Fixing the integration constants $C_i(\epsilon)$	13
5.3	Numerical consistency studies for set (11,12)	13
6	Result as a Power Series on z and $\log(z)$	14
7	Summary and outlook	16
A	Details on the ancillary file	18
A.1	Results for the individual contributions to the form factor B in electronic form	18
B	List of Master Integrals for diagrams 1 and 2	18
C	List of Master Integrals for diagrams 11 and 12	19

1 Introduction

The (weak) rare decays of B -mesons have been the focus point of theorists and experimentalists for some time, which is due to the potential they provide for the tests of the Standard Model (SM) at scales of several hundreds of GeV. Getting experimental information on rare decays puts strong constraints on the extensions of the SM, or can lead to disagreements with the SM predictions, providing evidence for new physics. To make a rigorous comparison between experiment and theory, one has to get refined theoretical predictions for the rare decay at hand. For the inclusive rare B -decays, the perturbative strong interaction effects result in sizable contributions.

In view of the expected increase in precision for the experimental measurements of the decay $B \rightarrow X_s \gamma$, a full next-to-next-to-leading logarithmic order (NNLL) calculation is necessary to reduce the theoretical uncertainties and to enable us to perform a rigorous comparison with existing and future experimental data. The first estimate of the branching ratio at $O(\alpha_s^2)$, leading to $\mathcal{B}(B \rightarrow X_s \gamma) = (3.15 \pm 0.23) \times 10^{-4}$, was done in [1], which is consistent with the experimental averages at the 1.2σ level. An updated version for this branching ratio, incorporating all results for NNLL contributions and lower-order perturbative corrections that have been calculated after 2006, was published in our paper [2]. For the CP- and isospin-averaged branching ratio we found $\mathcal{B}(B \rightarrow X_s \gamma) = (3.36 \pm 0.23) \times 10^{-4}$ which is in agreement with the current experimental averages.

It is well known that a part of the α_s^2 contributions in [2] was obtained via interpolation, i.e., using the results obtained through the large m_c asymptotic expansion on one hand and the results for $m_c = 0$ on the other hand. In the process of evaluating α_s^2 corrections directly at the physical value of m_c in [3], the part stemming from diagrams with closed fermion loops on gluon lines that contribute to the interference of the current-current and photonic dipole operators was calculated, extending previous work on such contributions [4].

The present paper is devoted to the computation of virtual α_s^2 corrections to the decay amplitude for $b \rightarrow s \gamma$ associated with the current-current operators¹ O_1 and O_2 , where we concentrate on contributions which do *not* involve closed fermion loops on gluon lines. The corresponding three-loop diagrams are rather complicated to calculate and we therefore divide the complete work into several (gauge invariant) classes of diagrams. In this paper we describe in detail our computational methods and explicitly work out those diagrams where no gluons are touching the b -quark line (see Figure 1).

The remainder of this paper is organized as follows: In section 2 we briefly present the theoretical framework and a few conventions. In section 3 we decompose the decay amplitude into form factors which can be written as linear combinations of scalar integrals (SIs); we then reduce the SIs to master integrals (MIs) and formulate differential equations for the latter.

¹The present paper is an extension of our old work on the corresponding α_s^1 corrections [5].

Furthermore we discuss that two methods are needed to work out the master integrals. In section 4 we present the method based on the canonical form of the differential equations which allows us to analytically work out the MIs for many diagrams. However, for four diagrams we did not manage to transform the corresponding MIs into canonical form. Therefore, in section 5, we present another method to compute these MIs which is based on an expansion in powers and logarithms of z ($z = m_c^2/m_b^2$) around $z = 0$. In section 6 we write the results for all diagrams calculated in this paper as an expansion on this type, retaining terms up to z^5 (and keeping all the accompanying powers of $\log(z)$). In section 7 we summarize our work and give a short outlook. The results for individual diagrams (or sets thereof) are submitted in electronic form together with the paper, as described in appendix A.1.

2 Theoretical framework

B -meson or b -quark decay amplitudes are usually calculated within the Weak Effective Theory (WET) where the SM particles with EW-scale masses have been integrated out. The WET lagrangian then contains QCD and QED interactions, and a tower of higher dimensional local operators which is typically truncated at dimension six [6,7]. The part of the WET Lagrangian which is relevant for the contributions discussed in this paper is:

$$\mathcal{L}_{\text{WET}} = \mathcal{L}_{\text{QCD}} + \mathcal{L}_{\text{QED}} + \frac{4G_F}{\sqrt{2}} V_{ts}^* V_{tb} \left[C_1 O_1 + C_2 O_2 + C_7 O_7 \right] \quad (2.1)$$

where

$$\begin{aligned} O_1 &= (\bar{s}\gamma_\mu P_L T^a c)(\bar{c}\gamma^\mu P_L T^a b) , & O_2 &= (\bar{s}\gamma_\mu P_L c)(\bar{c}\gamma^\mu P_L b) , \\ O_7 &= \frac{e}{16\pi^2} m_b (\bar{s}\sigma_{\mu\nu} P_R b) F^{\mu\nu} . \end{aligned} \quad (2.2)$$

We use the following conventions: $P_{R,L} = (1 \pm \gamma_5)/2$, $\sigma_{\mu\nu} \equiv (i/2)[\gamma_\mu, \gamma_\nu]$, the covariant derivative is given by $D_\mu q = (\partial_\mu + ieQ_q A_\mu + ig_s T^A G_\mu^A)q$, and $m_b = m_b(\mu)$ denotes the $\overline{\text{MS}}$ b -quark mass. In our calculation of order α_s^2 corrections from $O_{1,2}$, the scheme dependence of m_b is a higher order effect. Furthermore, we will neglect the strange quark mass throughout our paper.

3 Reduction of the decay amplitude to Master Integrals

In this section we briefly describe the *algebraic steps* which reduce the evaluation of a given three-loop diagram in Figure 1 to the computation of so-called Master Integrals (MIs). To this end, we decompose in section 3.1 the individual diagrams into form factors which can finally be represented as a linear combination of Scalar Integrals (SIs). In section 3.2 we decompose

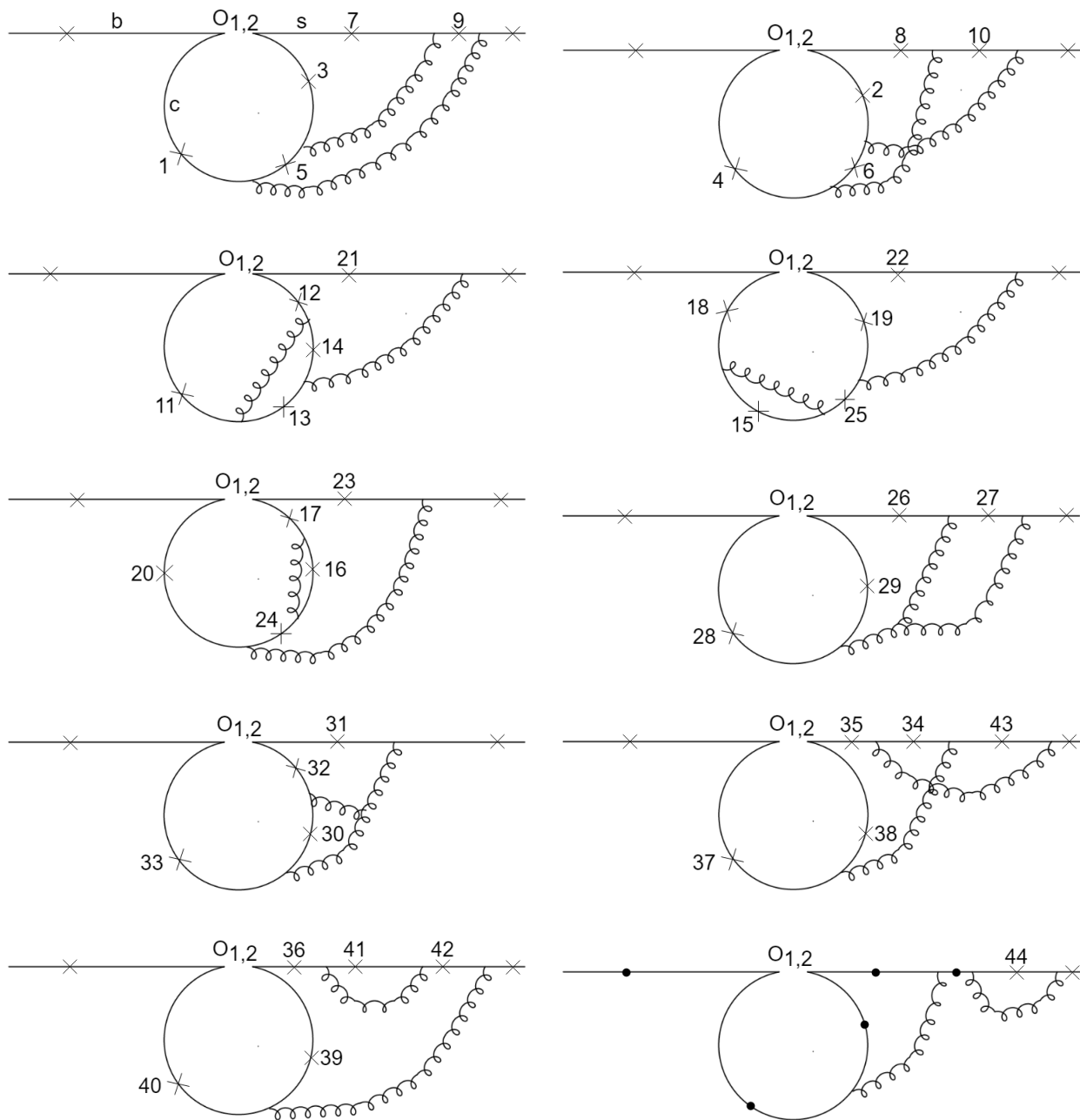


Figure 1: List of those three-loop contributions to $b \rightarrow s\gamma$ associated with O_1 and O_2 which are worked out in this paper. A cross or a dot on a quark line represents a possible place where the photon can be emitted. While the diagrams marked by a dot will be taken into account in a future work (in connection with renormalization), we worked out the effects on the $b \rightarrow s\gamma$ decay amplitude of all diagrams with numbered and unnumbered crosses in this figure. To this end, as discussed in detail in section 3.1, only the diagrams with numbered crosses had to be calculated explicitly.

these SIs into MIs. In section 3.3 we derive differential equations which govern the dependence on the charm quark mass of the MIs. In section 3.4 we briefly discuss our intention of how to calculate the MIs appearing in the various diagrams.

3.1 Form factor decomposition and scalar integrals

Using the standard Feynman rules in momentum space, the contribution to the decay amplitude $\mathcal{A}(b \rightarrow s\gamma)$ from a given Feynman diagram i in Figure 1 can be written as $\mathcal{A}^{(i)} = M_\mu^{(i)} \varepsilon^\mu$, where ε^μ denotes the polarization vector of the emitted photon. After performing purely algebraic manipulations like reductions of tensor integrals to scalar integrals (or alternatively using appropriate projection techniques) and freely using the equations of motion of the quark spinors and putting the strange quark mass to zero ($m_s = 0$), $M_\mu^{(i)}$ can be written in the form

$$M_\mu^{(i)} = \bar{u}_s(p_s) P_R [A^{(i)} q_\mu + B^{(i)} p_\mu + C^{(i)} \gamma_\mu] u_b(p). \quad (3.1)$$

In this equation $u_b(p)$ denotes the Dirac spinor of the b -quark with four-momentum p , $u_s(p_s)$ is the analogous quantity for the s -quark with four-momentum p_s and $q = p - p_s$ is the four-momentum of the emitted photon. At this level, the form factors $A^{(i)}$, $B^{(i)}$, $C^{(i)}$ are given in terms of linear combinations of scalar three-loop integrals. After performing these integrals and taking into account that $q^2 = 0$ in our process, these form factors are functions of m_b and m_c (and depend also on the renormalization scale μ).

Consider now a sum of diagrams which is gauge invariant with respect to QED. The quantity M_μ corresponding to this sum then satisfies $q^\mu M_\mu = 0$, leading to the relation $C = -\frac{m_b}{2} B$, where B and C denote form factors of the this sum. Using this relation, the corresponding gauge invariant amplitude $\mathcal{A} = M_\mu \varepsilon^\mu$ can then be written as

$$\mathcal{A} = -\frac{4\pi^2}{e m_b} B \langle O_7 \rangle_{\text{tree}}, \quad (3.2)$$

where the tree-level matrix element of the operator O_7 reads

$$\langle O_7 \rangle_{\text{tree}} = \frac{e m_b}{16\pi^2} \bar{u}_s(p_s) P_R [-4p_\mu + 2m_b \gamma_\mu] u_b(p) \varepsilon^\mu. \quad (3.3)$$

From eq. (3.2) we see that a gauge invariant amplitude \mathcal{A} can be written in such a way that only the form factor B appears. As the aim of our paper is to calculate the sum of all the diagrams in Figure 1, which is gauge invariant, it is sufficient to calculate only the form factors $B^{(i)}$ of each individual diagram i . It is easy to see that those diagrams in Figure 1 which are marked with a cross that does not carry a number, only would contribute to the form factors $C^{(i)}$. Therefore only the diagrams with numbered crosses (1-44) have to be worked out. A remark concerning the diagrams, where the photon emission is marked by a “dot”, is in order: We will take into account these contributions when working out the 2-loop counter-terms in a further publication.

We now discuss how to evaluate the scalar quantities $B^{(i)}$ for the three-loop diagrams listed in Figure 1. To have a concrete example let us have a look at diagrams 1 and 2 for which the momentum routings can be chosen such that the same propagators (i.e. denominators) appear which allows to sum these two diagrams from the very beginning. The results for the functions $B^{(i)}$ are given in terms of dimensionless three-loop scalar integrals of the type:

$$j[n_1, \dots, n_{12}] = (2\pi)^{-3d} \int \frac{(m_b^2)^{N-6} (\tilde{\mu}^2)^{3\epsilon} d^d \ell d^d r_1 d^d r_2}{P_1^{n_1} P_2^{n_2} P_3^{n_3} P_4^{n_4} P_5^{n_5} P_6^{n_6} P_7^{n_7} P_8^{n_8} P_9^{n_9} P_{10}^{n_{10}} P_{11}^{n_{11}} P_{12}^{n_{12}}} \quad (3.4)$$

where the numbers n_i are integers (positive or negative), with $N = \sum_{i=1}^{12} n_i$, the objects P_i are propagators (see below). In addition, $d = 4 - 2\epsilon$, and $\tilde{\mu}^2 \equiv \mu^2 e^{\gamma_E}/4\pi$, with μ the $\overline{\text{MS}}$ scale. Our choice of momentum routings fixes the first eight propagators, while the other four (sometimes called artificial propagators) are chosen such that the twelve propagators form a linearly-independent set (in the sense that all occurring scalar products involving only loop-momenta or scalar products between loop-momenta and external momenta can be written as a linear combination of these propagators). Explicitly, the complete list of propagators needed for diagrams 1 and 2 reads:

$$\begin{aligned} P_1 &= (\ell + q)^2 - m_c^2, & P_2 &= \ell^2 - m_c^2, & P_3 &= (\ell + r_2)^2 - m_c^2, \\ P_4 &= (\ell + r_1 + r_2)^2 - m_c^2, & P_5 &= r_1^2, & P_6 &= r_2^2, \\ P_7 &= (r_2 + p_s)^2, & P_8 &= (r_1 + r_2 + p_s)^2, & P_9 &= (r_1 + r_2)^2, \\ P_{10} &= (\ell + p_s)^2, & P_{11} &= (r_1 + q)^2, & P_{12} &= (r_2 + q)^2. \end{aligned} \quad (3.5)$$

Returning to the complete list of diagrams in Figure 1, we define the following sets of diagrams, in order to economize our calculation: (1, 2), (3, 4), (5, 6), (7, 8), (9, 10), (11, 12), (13, 14), (15, 16, 17, 18), (19, 20), (21, 22, 23), (24, 25), (26), (27), (28, 29), (30), (31), (32, 33), (34), (35, 36), (37, 38, 39, 40), (41, 42) and (43, 44). In a given set the momentum routings can be chosen in such a way that the same propagators appear, allowing to sum the diagrams in this set from the very beginning. In the ancillary file submitted together with the present paper, we will give for each set j the corresponding form factor contribution $B^{(j)}$. In the following we describe the analytic calculation of the three-loop scalar integrals.

3.2 IBP reduction and Master integrals

At this point, the result for a given set j of diagrams is a linear combination of many scalar integrals. We can now apply integration-by-parts identities (IBPs) to reduce the scalar integrals to a small set of *Master Integrals* (MIs). For this purpose we use the code KIRA [8, 9] which implements Laporta's algorithm [10]. In earlier stages of our work also the program LiteRed [11] was used.

After reduction, we are left with N three-loop MIs for the considered set. For example, for set (1, 2) we get the MIs J_i ($i = 1, \dots, 27$), which are listed in Appendix B.

We now perform some simplifying operations on the master integrals. First, we express the integrands in terms of the dimensionless variable

$$z \equiv m_c^2/m_b^2. \quad (3.6)$$

Second, in order to do a rational transformation to a canonical basis of master integrals whenever possible, we make a change of variable $z \mapsto x$, where $x = x(z)$ is a function to be specified later. In terms of this new variable the dimensionless MIs are denoted as $J_i(\epsilon, x)$.

3.3 Differential equations for the Master integrals

For a given set we first construct the system of differential equations for the MIs:

$$\partial_x J_k(\epsilon, x) = a^{k\ell}(\epsilon, x) J_\ell(\epsilon, x), \quad (3.7)$$

where \mathbf{a} is a $N \times N$ matrix depending on ϵ and x . The derivatives of the MIs J_k are performed by differentiating the integrands, which produce new scalar integrals, and then applying the IBP reduction again on these scalar integrals to express the derivatives $\partial_x J_k$ themselves in terms of the MIs J_k . One can then read off the matrix \mathbf{a} .

3.4 Methods used to calculate the Master Integrals

For all sets except (11, 12) and (13, 14), we managed to transform the corresponding differential equations into canonical form. These canonical equations can then be iteratively solved as an expansion in the dimensional regulator ϵ . In these solutions the dependence on the charm-quark mass is contained in Generalized Polylogarithms (GPLs). In each iteration step new integration constants come into the game. The details for computation of the MIs for these diagrams (including comments about fixing the integration constants) are presented in section 4. We stress that this method is purely analytic and therefore the preferred one.

For the MIs in sets (11, 12) and (13, 14), however, we did not manage to find a transformation to a canonical basis. We therefore used another method by performing a series expansion at $z = 0$ (i.e., in terms of powers and logarithms of $z = m_c^2/m_b^2$). This method is described in some details in section 5.

4 Solving MIs via canonical form

In this section we explain the details of the calculation of the MIs whose differential equations can be transformed to canonical form (i.e., the MIs of all sets except (11, 12) and (13, 14)).

4.1 Canonical form and iterative solution

Adapted to our situation where the MIs depend (besides the dimensional regulator ϵ) only on one variable x , a basis of MIs is said to be “canonical” [12] if $\mathbf{a}(\epsilon, x) = \epsilon \mathbf{A}(x)$, with $\mathbf{A}(x)$ being a $N \times N$ matrix independent of ϵ . Given a canonical basis \vec{M} , the differential equation has the form²:

$$\partial_x \vec{M}(\epsilon, x) = \epsilon \mathbf{A}(x) \vec{M}(\epsilon, x) \quad . \quad (4.1)$$

Once a canonical basis is found, the system of differential equations can be solved automatically order by order in ϵ . To keep the notation as simple as possible in this section, we will assume that all the master integrals in the canonical basis are regular in ϵ (if not, we redefine them by multiplying all of them with the same appropriate power of ϵ). We then write the ϵ -expansion for the master integrals

$$\vec{M}(\epsilon, x) = \sum_{n=0}^{\infty} \epsilon^n \vec{M}_n(x) \quad (4.2)$$

and the differential equation reads:

$$\partial_x \vec{M}_n(x) = \mathbf{A}(x) \vec{M}_{n-1}(x) \quad . \quad (4.3)$$

Using partial fraction decomposition, \mathbf{A} can be written in the form

$$\mathbf{A}(x) = \sum_j \frac{\mathbf{A}^j}{x - w_j} \quad , \quad (4.4)$$

where \mathbf{A}^j is a set of constant matrices, and the quantities w_j are called the “weights”, which in our application are just constants.

The differential equation (4.3) can be solved iteratively: As $\vec{M}_{-1}(x) = 0$ (see eq. (4.2) and the text before this equation), (4.3) implies that $\vec{M}_0(x)$ is constant, i.e., $\vec{M}_0(x) = \vec{C}_0$. From $\vec{M}_0(x)$, we can get $\vec{M}_1(x)$ by just integrating (4.3) for $n = 1$ with respect to x . This step brings in a new integration constant \vec{C}_1 . Repeating this procedure, we get

$$\begin{aligned} \vec{M}_0(x) &= \vec{C}_0 \quad , \\ \vec{M}_1(x) &= \sum_{j_1} [\mathbf{A}^{j_1} G(w_{j_1}; x)] \vec{C}_0 + \vec{C}_1 \quad , \\ \vec{M}_2(x) &= \sum_{j_2, j_1} [\mathbf{A}^{j_2} \mathbf{A}^{j_1} G(w_{j_2}, w_{j_1}; x)] \vec{C}_0 + \sum_{j_2} [\mathbf{A}^{j_2} G(w_{j_2}; x)] \vec{C}_1 + \vec{C}_2 \quad , \\ \vec{M}_3(x) &= \dots \end{aligned} \quad (4.5)$$

²A similar presentation is given in our paper [13] for the case where the MIs depend on two variables x and y .

etc., in terms of Generalized Polylogarithms (GPLs) [14], defined iteratively as [15]

$$G(w_1, \dots, w_n; x) = \int_0^x \frac{dt}{t - w_1} G(w_2, \dots, w_n; t); \quad G(; x) = 1; \quad G(\vec{0}_n; x) = \frac{\log^n x}{n!}, \quad (4.6)$$

where $\vec{0}_n$ denotes n consecutive zeroes.

Thus, the problem of calculating the MIs is reduced to find a canonical basis and to fix the integration constants, which is a much more tractable challenge. In order to find canonical master integrals, we used the mathematica program *CANONICA* [16] (and for some checks also the program *Libra* [24]). The *CANONICA* code is able to look for transformations that involve *rational* functions of the argument x . For this reason, the “right” variable x must be found before using this program. Starting from our original variable $z = m_c^2/m_b^2$, we define x as

$$x = \frac{1}{\sqrt{1 - 4z}} \quad (4.7)$$

in all sets considered in this paper. In terms of this variable and with the help of *CANONICA*, we are able to find linear transformations

$$M_k = (T^{-1})^{k\ell}(\epsilon, x) J_\ell, \quad (4.8)$$

such that the MIs M_k constitute a canonical basis. The weights occurring in the considered sets read:

$$w_0 = 0, w_1 = 1, w_2 = -1, w_3 = \frac{i}{\sqrt{3}}, w_4 = -\frac{i}{\sqrt{3}}, w_5 = \frac{1}{\sqrt{5}}, w_6 = -\frac{1}{\sqrt{5}}. \quad (4.9)$$

We stress that the chosen variable x has the property that it tends to zero when z goes to infinity. In this limit, the functions $G(\dots; x)$ can be expanded in a straightforward way for small values of x . This turns out to be very useful when fixing the integration constants in the following section, because we will heavily make use of the asymptotic properties of the originals integrals J_k in the limit where x goes to zero.

4.2 Fixing integration constants

Once the canonical basis is found for a given set of diagrams and the general solution of the differential equations in this basis is constructed, we have to fix the integration constants. To this end we transform in a first step the MIs \vec{M} back to the original basis consisting of the MIs J_k by making use of the transformation matrix T (i.e. Eq. (4.8)). The constants are then determined by computing some of the simpler MIs J_k in a traditional way (i.e. through Feynman parametrization), while for the more difficult MIs asymptotic properties in the limit $z \rightarrow \infty$ can be worked out. These properties follow in a straightforward way from the heavy mass expansion (HME) of a given integral [17].

To be somewhat more concrete, we briefly explain which properties/statements were used to fix the constants for the 27 MIs appearing in the set (1, 2) (see equations (B.4) and (3.5)):

1. J_1 and J_2 can easily be worked out traditionally.
2. In the limit for large m_c ($m_c \gg m_b$) the other 25 integrals can be naively Taylor expanded in the external momenta and in m_b . Note that in set (1, 2) the only contributing subdiagrams of the MIs in the sense of the HME are just the full diagrams (i.e. the full MIs) and therefore the naive Taylor expansion is justified. The leading power (i.e. the maximal power) in the large m_c -expansion of a given integral J_k is then of the form $m_c^{n-6\epsilon}$, where the integer n is identical to the mass dimension of the integral (strictly speaking of the integral in which the factor $(m_b^2)^{N-6}(\tilde{\mu}^2)^{3\epsilon}$ in the definition (3.4) is understood to be omitted); the structure of J_k is

$$J_k = K m_c^{n-6\epsilon} P(m_b^2/m_c^2), \quad (4.10)$$

where K is a constant prefactor (w.r.t. m_c) and P is a polynomial of the indicated argument. The GPLs in the general solution for the MIs (from the differential equations) can easily be expanded for large z . Very often, the expanded solution for a given integral contains higher powers in m_c than that determined from the HME argumentation. The requirement that these terms are absent allows to determine some of the integration constants. From the HME structure it is also clear that n in equation (4.10) is an *even* integer; this information again fixes some of the integration constants.

3. The leading power in m_c of the MI J_6 (which scales like $m_c^{4-6\epsilon}$ in the large m_c limit) coincides with J_2 .
4. The HME of the MI J_{23} produces only the following powers of m_c : $m_c^{n-6\epsilon}$, where n is an integer in the range $n = 2, 0, -2, -4, \dots$. Therefore, when multiplying J_{23} with $m_c^{+6\epsilon}$ and then expanding in ϵ , there can be no logarithms in m_c . This property fixes the remaining constants in set (1, 2).

It is worth emphasizing that in set (1, 2) all constants can be fixed by the explicit knowledge of J_1 and J_2 and structural information resulting from HME on the (integer parts) of the powers of m_c and on the logarithms in m_c . *The explicit HME evaluation of the MIs is not even necessary.*

For many other sets of diagrams the fixing of the integration constants works in a similar way. However, in some sets the HME of certain MIs requires to analyze genuine subdiagrams which make the extraction of the constants somewhat more complicated. Furthermore, in set (21, 22, 23) a three-loop tadpole integral with four charm-lines appears which we could not calculate analytically; we took the results from [18] where this integral was calculated numerically to very high precision. To close this section, we note that our final results for all MIs have been checked numerically using Sector Decomposition as implemented in SecDec [19] or PySecDec [20].

4.3 Expansion around $z = 0$

The MIs of all sets (except (11,12) and (13,14)) are now given in terms of GPLs and all the integrations constants are fixed. However, the corresponding expressions are lengthy and the numerical evaluation (for example using GiNaC [21–23]) of the large number of GPLs is time-consuming. We therefore decided to expand all GPLs around $z = 0$ (leading to powers and logarithms of z). Needless to say, the physical value of $z \sim 0.1$ is considerably smaller than 0.25, corresponding to the radius of convergence of this expansion. Using the expanded versions of the MIs, we worked out the form factor contributions $B^{(i)}$ for the individual sets i of diagrams. The results for these $B^{(i)}$ quantities, consistently expanded up to the power z^{10} (and including all power of $\log(z)$), can be found in the mathematica file “ancillary.m” which is submitted together with this paper (for details see Appendix A.1).

5 Calculating the MIs in sets (11, 12) and (13, 14)

5.1 Solving the differential equations as an expansion for small z

As we already mentioned in section 3.4, we could not find transformations of the MIs J_k to a canonical basis for the sets (11, 12) and (13, 14), and therefore we propose another method for these two sets. As the physical value of $z = m_c^2/m_b^2$ is a small parameter (actually of order 0.1), we construct a series expansion for the solutions around $z = 0$. We start with the differential equation in matrix form as

$$\partial_z \vec{J}(\epsilon, z) = A(\epsilon, z) \vec{J}, \quad (5.1)$$

where $A(\epsilon, z)$ is an $N \times N$ matrix (N is the number of MIs) which depends on z and ϵ in a rational way. First of all we transform the differential equation into Fuchsian form (see e.g. [24]), i.e. in such a way that the transformed version of A has at most $1/z$ singularities in all entries. This can be achieved by transforming $\vec{J} \mapsto \vec{J}' = L^{-1} \vec{J}$ with a diagonal matrix L with entries of the form $L_{ii} = z^{n_i}$, where n_i are suitably chosen integers. The transformed matrix, denoted by A_1 then reads

$$A_1 = \frac{\partial L^{-1}}{\partial z} L + L^{-1} A L. \quad (5.2)$$

By construction, the singular part of A_1 , denoted by A_s , is then proportional to $\frac{1}{z}$. In the next step we apply a further transformation $\vec{J}' \mapsto \vec{J}'' = S^{-1} \vec{J}'$ which brings A_s to Jordan form, i.e. to a matrix with upper triangular form, for which only the elements on the diagonal and above the diagonal are nonzero. Practically, this is done in Mathematica, using the command $S = \text{JordanDecomposition}[A_s][[1]]$. Note that S depends on ϵ , but not on z . The MIs \vec{J}'' then obey the differential equation

$$\partial_z \vec{J}'' = A_2(\epsilon, z) \vec{J}'' \quad \text{with} \quad A_2 = S^{-1} A_1 S. \quad (5.3)$$

The N coefficients $C_i(\epsilon)$ play the role of integration constants, which we will fix below by exploiting suitable information extracted from the integral representations of the MIs near $z = 0$. We note that so far no expansion in ϵ was performed. Also note that the MIs \vec{J} are known with a maximum power of z which is less than n_{\max} , because the back transformation matrix L contains terms proportional $\frac{1}{z^i}$ with positive i .

5.2 Fixing the integration constants $C_i(\epsilon)$

We briefly describe how to fix the integration constants $C_i(\epsilon)$ which appear in Eq. (5.6). To this end, it is convenient to cast this equation in component form:

$$J_k = \sum_{i=1}^N C_i(\epsilon) J_{i,k}. \quad (5.7)$$

Note that the ϵ dependence of the fundamental solutions $J_{i,k}$ on the right hand side of this equation is still exact (i.e. not expanded), while the z -dependence is contained in terms of the form

$$z^{n-m_0\epsilon}, \quad z^{n-m_0\epsilon} \log(z), \quad z^{n-m_0\epsilon} \log^2(z), \quad (5.8)$$

where n is a non-negative integer and $m_0 = 0, 1, 2, 3, 4$. For each J_k we now build a leading power version J_k^{lead} by keeping for any given m_0 only all the terms with the smallest n .

To gain information on the integration constants, we use *the method of regions* (see e.g. [25–27]), in particular the version formulated in Feynman- or α -parameter space as described in sections 9.2 and 9.3 in [26, 27], respectively. This version is implemented in the program FIESTA5 [28] (which we mainly called with the QMC integrator [29]; for checks we also called FIESTA5 with the VEGAS integrator [30]). This program (after some minor adaptations done by us) allows to numerically calculate the leading versions of the MIs J_k directly from their integral representations. For many MIs we could check specific regions even analytically by using the program HyperInt [31].

The requirement that the leading versions of the left- and the right-hand side of Eq. (5.7) coincide, fixes the integration constants.

5.3 Numerical consistency studies for set (11,12)

In this section we investigate a few aspects of the form factor contribution $B_{(11,12)}$ corresponding to the set (11, 12). We write this contribution as

$$B_{(11,12)} = \text{pref} \cdot \hat{B} \quad \text{with} \quad \text{pref} = -\frac{e m_b}{4\pi^2} g_s^4 \left(\frac{\mu^2}{m_b^2} \right)^{3\epsilon}. \quad (5.9)$$

Figure 2 shows the dimensionless quantity \hat{B} , where the solid curves are obtained as described in sections 5.1 and 5.2. The results for negative values of z are related to those for positive

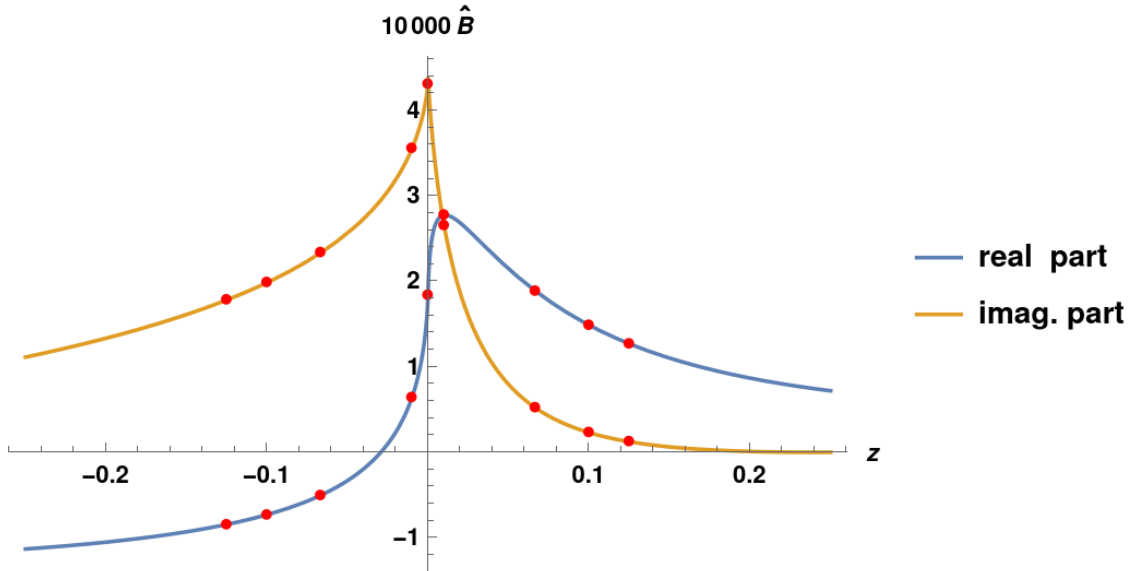


Figure 2: Form factor contribution $10^4 \times \hat{B}$ as defined in Eq. (5.9). See text for details.

z (i.e. physical values) via analytic continuation through the lower z -half-plane. As a consistency check, we calculated \hat{B} for the values $z = 1/100$, $z = 1/15$, $z = 1/10$ and $z = 1/8$ by directly working out the 31 MIs numerically at these values for z using SecDec and/or PySecDec (without using method by region features). These results are shown by red dots in Figure 2. Furthermore, we did a similar direct numerical calculation using FIESTA5 for the corresponding negative values for z (again without using method by region features). These results are also shown by red dots in Figure 2. Finally, we did a completely new calculation by putting $z = 0$ from the very beginning. In this case, the form factor contribution \hat{B} is given in terms of only 3 MIs, viz. J_7 , J_{18} and J_{25} (see Eq. (C.6)), which we calculated for $m_c = 0$ using SecDec. The corresponding result is also shown by a dot. We think that Figure 2 nicely shows the intrinsic consistency of our approach.

6 Result as a Power Series on z and $\log(z)$

In this paper we worked out the contributions to the $b \rightarrow s\gamma$ decay amplitude of all three-loop diagrams in Figure 1 which are marked with crosses (both numbered and unnumbered crosses). We denote the contributions related to the operators O_1 and O_2 as \mathcal{A}_1 and \mathcal{A}_2 , respectively. These diagrams form a gauge invariant set (w.r.t. to QED) and therefore, as detailed in section 3.1, it is sufficient to explicitly calculate the form factor B (see Eq. (3.2)) to which only the diagrams with numbered crosses contribute. While the form factor contributions $B^{(i)}$ from the individual sets of diagrams are given in electronic form in the file “ancillary.m” (see Appendix A.1), we give here the results for \mathcal{A}_1 and \mathcal{A}_2 as power series on z where we list terms up to z^5 .

$O_1, \frac{1}{\epsilon}$	z^0	z^1	z^2	z^3	z^4	z^5
$\log(z)^0$	$0.298 + 0.255I$	$1.047 - 1.616I$	$0.733 + 3.407I$	$-1.441 - 3.546I$	$-0.390 - 0.258I$	$-0.224 - 1.412I$
$\log(z)^1$	0	$0.834 - 1.138I$	$2.870 - 0.550I$	$-1.268 + 1.300I$	$-0.0821 - 0.0111I$	$-0.449 - 0.0691I$
$\log(z)^2$	0	$-0.240 - 0.653I$	$-0.0875 - 0.852I$	$0.207 + 0.0664I$	-0.00176	-0.0110
$\log(z)^3$	0	$-0.0693 + 0.0187I$	-0.0904	0.00704	0	0
$\log(z)^4$	0	0.00148	0	0	0	0
$\log(z)^5$	0	0	0	0	0	0

Table 1: Numerical values for $10^3 \times c^{(1,-1)}$ (see equation (6.10)).

O_1, ϵ^0	z^0	z^1	z^2	z^3	z^4	z^5
$\log(z)^0$	$0.0702 + 0.281I$	$1.248 - 0.655I$	$-3.087 + 1.928I$	$4.573 - 1.446I$	$-1.544 - 1.130I$	$2.270 - 1.244I$
$\log(z)^1$	0	$0.444 - 0.0479I$	$1.128 + 0.958I$	$-1.392 - 1.805I$	$-0.0765 + 1.372I$	$-0.201 - 1.063I$
$\log(z)^2$	0	$-0.033 - 0.158I$	$-0.257 - 0.162I$	$-0.0339 + 0.261I$	$0.360 - 0.0760I$	$-0.185 - 0.0401I$
$\log(z)^3$	0	$-0.001 + 0.099I$	$0.00390 + 0.164I$	$0.00704 - 0.0334I$	$-0.00789 - 0.0412I$	$-0.00315 + 0.0265I$
$\log(z)^4$	0	$0.0131 - 0.000829I$	$0.0198 - 0.00296I$	-0.00318	-0.00328	0.00211
$\log(z)^5$	0	-0.000142	-0.000188	0	0	0

Table 2: Numerical values for $10^2 \times c^{(1,0)}$ (see equation (6.10)).

For a given power of z we retain all powers of $\log(z)$, which practically means up to $\log^5(z)$ as there are no higher log-powers. The results read (for $k = 1, 2$)

$$\mathcal{A}_k = g_s^4 \left(\frac{\mu^2}{m_b^2} \right)^{3\epsilon} \langle O_7 \rangle_{\text{tree}} \left[\frac{c^{(k,-2)}}{\epsilon^2} + \sum_{i=0}^5 \sum_{j=0}^5 \left(\frac{1}{\epsilon} c_{ij}^{(k,-1)} + c_{ij}^{(k,0)} \right) z^i \log(z)^j \right], \quad (6.10)$$

where $c^{(1,-2)} = 0.00002701 + 0.000006681 z$, $c^{(2,-2)} = -0.0001115 - 0.00004008 z$, and $c_{ij}^{(1,-1)}$, $c_{ij}^{(1,0)}$, $c_{ij}^{(2,-1)}$, $c_{ij}^{(2,0)}$ are given in Tables 1,2,3 and 4. We mention that the reader can easily obtain results for \mathcal{A}_1 and \mathcal{A}_2 up to the z^{10} by using the information in the file ‘‘ancillary.m’’. The results when going up to z^5 and those when going up to z^{10} are close to each other, for instance for $z = 1/8$ the relative difference is only of order 0.5%.

$O_2, \frac{1}{\epsilon}$	z^0	z^1	z^2	z^3	z^4	z^5
$\log(z)^0$	$-1.227 - 1.051I$	$-4.920 + 7.970I$	$-4.460 - 17.128I$	$7.240 + 18.141I$	$2.066 + 1.436I$	$1.157 + 7.770I$
$\log(z)^1$	0	$-3.441 + 5.822I$	$-14.052 + 3.298I$	$6.608 - 6.454I$	$0.457 + 0.0664I$	$2.473 + 0.415I$
$\log(z)^2$	0	$1.278 + 2.912I$	$0.525 + 4.106I$	$-1.027 - 0.398I$	0.0106	0.066
$\log(z)^3$	0	$0.309 - 0.112I$	0.436	-0.0422	0	0
$\log(z)^4$	0	-0.0089	0	0	0	0
$\log(z)^5$	0	0	0	0	0	0

Table 3: Numerical values for $10^3 \times c^{(2,-1)}$ (see equation (6.10)).

O_2, ϵ^0	z^0	z^1	z^2	z^3	z^4	z^5
$\log(z)^0$	$-0.330 - 1.157I$	$-2.922 + 2.250I$	$1.091 - 6.952I$	$0.0581 + 1.884I$	$-16.856 + 5.502I$	$3.643 + 10.932I$
$\log(z)^1$	0	$-1.284 - 1.243I$	$-5.118 + 2.733I$	$-1.066 - 6.449I$	$1.349 + 11.105I$	$3.797 - 7.035I$
$\log(z)^2$	0	$0.107 + 0.0505I$	$2.071 + 1.250I$	$-2.180 + 1.694I$	$2.752 - 0.124I$	$-2.469 - 0.441I$
$\log(z)^3$	0	$-0.120 - 0.515I$	$0.193 - 0.671I$	$0.282 + 0.131I$	$-0.0142 - 0.335I$	$-0.0534 + 0.311I$
$\log(z)^4$	0	$-0.0642 + 0.0162I$	$-0.0861 - 0.0271I$	0.0136	-0.0267	0.0248
$\log(z)^5$	0	0.00156	-0.00172	0	0	0

Table 4: Numerical values for $10^2 \times c^{(2,0)}$ (see equation (6.10)).

7 Summary and outlook

In this paper we worked out three-loop diagrams (of order α_s^2) contributing to the decay amplitude for $b \rightarrow s\gamma$ associated with the current-current operators O_1 and O_2 at the physical value of m_c . As the corresponding calculations are among the hardest we have ever done, we concentrated only on the well-defined class of diagrams where no gluon is touching the b -quark line (see Figure 1) in this paper; note that we did not work out the diagrams with closed fermion bubbles inserted into gluon-lines, because these contributions already exist in the literature. For many diagrams we could solve the master integrals using differential equations in the canonical form, as presented in section 4. However, for the four diagrams (11 – 14) we could not find a transformation to canonical form and we therefore calculated in section 5 the corresponding master integral directly as an expansion around $z = 0$, retaining power terms up to z^{10} and keeping the accompanying $\log(z)$ terms to all powers. The results for the sum of all considered diagrams are given in tabular form in section 6 and also in electronic form in the file ancillary.m, which is submitted together with this paper (see Appendix A.1). Making use of the two methods discussed in this paper, we are confident that we will manage to work out the remaining three-loop diagrams (at the physical value of m_c), completing the virtual QCD corrections of order α_s^2 to the decay amplitude $\mathcal{A}(b \rightarrow s\gamma)$ associated with O_1 and O_2 .

Acknowledgements

C.G. is very grateful to G. Heinrich, V. Magerya, J. Schlenk, and especially to S. Jones, for useful discussions on SecDec and PySecDec, in particular on the “method by regions” features. He also acknowledges useful discussions with Christoph Meyer on his program CANONICA as well as discussions with Johann Usovitsch on finding a “good bases” of master integrals with his program factorizeBasis.nb which extends KIRA. Further thanks go to R.N. Lee for questions on his programs LiteRed and Libra. C.G. also would like to thank J. Gasser for lecturing (a long time ago) about Fuchsian equations in his courses on quantum mechanics. Also very useful discussions with N. Schalch on various features connected with multiloop

diagrams are gratefully acknowledged.

The work of C.G., C.W. and F.S. is partially supported by the Swiss National Science Foundation under grants 200020-175449 and 200020-204075.

H.M.A. is supported by the Committee of Science of Armenia Program Grant No. 21AG-1C084.

A Details on the ancillary file

A.1 Results for the individual contributions to the form factor B in electronic form

In the mathematica-file “ancillary.m” (which is included in the submission of this paper) we give the contributions to the form factor B (see Eq. (3.1)) for the following 22 sets of diagrams: (1, 2), (3, 4), (5, 6), (7, 8), (9, 10), (11, 12), (13, 14), (15, 16, 17, 18), (19, 20), (21, 22, 23), (24, 25), (26), (27), (28, 29), (30), (31), (32, 33), (34), (35, 36), (37, 38, 39, 40), (41, 42) and (43, 44). In this file, the contributions from sets (1, 2) and (37, 38, 39, 40) are denoted as “B1to2” and “B37to40”, respectively (and so on). The expressions contain the results as an expansion in z (around $z = 0$), where terms up to z^{10} are retained. Note that for a given power of z all powers of $\log(z)$ are kept. The formulas contain the symbolic prefactor “pref”, which amounts to

$$\text{pref} = -\frac{e m_b}{4\pi^2} g_s^4 \left(\frac{\mu^2}{m_b^2} \right)^{3\epsilon}, \quad (\text{A.1})$$

as well as symbolic color-factors “col[i]”. The actual values for these color-factor are also given in this file for both, the O_1 - and the O_2 -contributions; they are given as mathematica-lists denoted by “coloro1” and “coloro2”, being written in terms of the number of colors N_c ($N_c = 3$). If the form factor contributions related to O_1 are of interest, the following replacement should be done (e.g. in the mathematica notebook into which the ancillary file is imported):

$$\text{col}[i_] := \text{coloro1}[[i]] \quad (\text{A.2})$$

Furthermore the formulas contain the symbolic charge-factors Q_c and Q_s (whose numerical values are $Q_c = 2/3$ and $Q_s = -1/3$).

According to section 3.1, the decay amplitude corresponding to the diagrams considered in this paper (see Figure 1) is obtained through

$$\mathcal{A}_k = -\frac{4\pi^2}{e m_b} B_k \langle O_7 \rangle_{\text{tree}} \quad (k = 1, 2), \quad (\text{A.3})$$

where B_k is the sum of the 22 form factor contributions associated with the operator O_k ($k = 1, 2$). In order to check that the ancillary file works properly, the reader is invited to reproduce the coefficients in Eq. (6.10) (which are given in Tables 1, 2, 3 and 4).

B List of Master Integrals for diagrams 1 and 2

In this appendix we list the Master Integrals (MIs) J_1, \dots, J_{27} which appear in the calculation of the three-loop diagrams 1 and 2 contained in Figure 1. The notation is described in equation (3.4) and the explicit form of the propagators is given in equation (3.5).

The 27 MIs read:

$$\begin{aligned}
J_1 &= j[1, 0, 1, 1, 0, 0, 0, 0, 0, 0, 0] & J_2 &= j[1, 0, 0, 1, 1, 1, 0, 0, 0, 0, 0] \\
J_3 &= j[1, 0, 1, 1, 0, 0, 1, 0, 0, 0, 0] & J_4 &= j[1, 0, 1, 1, 0, 0, 2, 0, 0, 0, 0] \\
J_5 &= j[1, 1, 1, 1, 0, 0, 1, 0, 0, 0, 0] & J_6 &= j[1, 0, 0, 1, 1, 0, 1, 0, 0, 0, 0] \\
J_7 &= j[1, 0, 0, 1, 1, 0, 2, 0, 0, 0, 0] & J_8 &= j[1, 0, 0, 2, 1, 0, 1, 0, 0, 0, 0] \\
J_9 &= j[1, 1, 0, 1, 1, 1, 1, 0, 0, 0, 0] & J_{10} &= j[1, 0, 1, 1, 0, 1, 0, 1, 0, 0, 0] \\
J_{11} &= j[1, 0, 1, 1, 0, 1, 0, 2, 0, 0, 0] & J_{12} &= j[1, 0, 1, 1, 0, 2, 0, 1, 0, 0, 0] \\
J_{13} &= j[1, 0, 1, 2, 0, 1, 0, 1, 0, 0, 0] & J_{14} &= j[1, 0, 2, 1, 0, 1, 0, 1, 0, 0, 0] \\
J_{15} &= j[1, 0, 0, 1, 1, 1, 0, 1, 0, 0, 0] & J_{16} &= j[1, 0, 0, 1, 1, 1, 0, 2, 0, 0, 0] \\
J_{17} &= j[1, 1, 0, 1, 1, 1, 0, 1, 0, 0, 0] & J_{18} &= j[1, 0, 1, 1, 1, 1, 0, 1, 0, 0, 0] \\
J_{19} &= j[1, 0, 1, 1, 1, 1, 0, 2, 0, 0, 0] & J_{20} &= j[1, 0, 1, 1, 1, 2, 0, 1, 0, 0, 0] \\
J_{21} &= j[1, 0, 1, 1, 2, 1, 0, 1, 0, 0, 0] & J_{22} &= j[1, 1, 1, 1, 1, 1, 0, 1, 0, 0, 0] \\
J_{23} &= j[1, 0, 1, 1, 0, 0, 1, 1, 0, 0, 0] & J_{24} &= j[1, 0, 1, 1, 0, 0, 1, 2, 0, 0, 0] \\
J_{25} &= j[1, 0, 1, 2, 0, 0, 1, 1, 0, 0, 0] & J_{26} &= j[1, 1, 1, 1, 0, 0, 1, 1, 0, 0, 0] \\
J_{27} &= j[1, 0, 1, 1, 0, 1, 1, 1, 0, 0, 0] & &
\end{aligned} \tag{B.4}$$

C List of Master Integrals for diagrams 11 and 12

In this appendix we list the Master Integrals (MIs) J_1, \dots, J_{31} which appear in the calculation of the three-loop diagrams 11 and 12 contained in Figure 1. The set of propagators reads (where again the first eight are physical and the remaining four are artificial):

$$\begin{aligned}
P_1 &= \ell^2 - m_c^2, & P_2 &= (\ell + q)^2 - m_c^2, & P_3 &= (\ell + r_1)^2 - m_c^2, \\
P_4 &= (\ell + r_2)^2 - m_c^2, & P_5 &= (\ell + r_1 + r_2)^2 - m_c^2, & P_6 &= r_1^2, \\
P_7 &= r_2^2, & P_8 &= (r_1 + p_s)^2, & P_9 &= (\ell + p_s)^2, \\
P_{10} &= (r_1 + q)^2, & P_{11} &= (r_2 + q)^2, & P_{12} &= (r_2 + p_s)^2.
\end{aligned} \tag{C.5}$$

The 31 MIs read:

$$\begin{aligned}
J_1 &= j[1, 0, 1, 1, 0, 0, 0, 0, 0, 0, 0] & J_2 &= j[1, 0, 1, 1, 1, 0, 0, 0, 0, 0, 0] \\
J_3 &= j[0, 0, 1, 1, 0, 1, 1, 0, 0, 0, 0] & J_4 &= j[0, 1, 1, 1, 0, 0, 0, 1, 0, 0, 0] \\
J_5 &= j[0, 1, 1, 1, 0, 0, 0, 2, 0, 0, 0] & J_6 &= j[1, 1, 1, 1, 0, 0, 0, 1, 0, 0, 0] \\
J_7 &= j[0, 1, 1, 1, 1, 0, 0, 1, 0, 0, 0] & J_8 &= j[0, 1, 1, 1, 1, 0, 0, 2, 0, 0, 0] \\
J_9 &= j[0, 1, 1, 1, 2, 0, 0, 1, 0, 0, 0] & J_{10} &= j[0, 1, 2, 1, 1, 0, 0, 1, 0, 0, 0] \\
J_{11} &= j[1, 1, 1, 1, 1, 0, 0, 1, 0, 0, 0] & J_{12} &= j[1, 1, 1, 1, 2, 0, 0, 1, 0, 0, 0] \\
J_{13} &= j[0, 1, 1, 1, 0, 0, 1, 1, 0, 0, 0] & J_{14} &= j[0, 1, 1, 1, 0, 0, 1, 2, 0, 0, 0] \\
J_{15} &= j[0, 1, 1, 1, 0, 0, 2, 1, 0, 0, 0] & J_{16} &= j[0, 1, 1, 2, 0, 0, 1, 1, 0, 0, 0] \\
J_{17} &= j[0, 1, 2, 1, 0, 0, 1, 1, 0, 0, 0] & J_{18} &= j[0, 1, 0, 0, 1, 0, 1, 1, 0, 0, 0] \\
J_{19} &= j[0, 1, 0, 0, 1, 0, 1, 2, 0, 0, 0] & J_{20} &= j[0, 1, 0, 0, 2, 0, 1, 1, 0, 0, 0] \\
J_{21} &= j[0, 1, 0, 1, 1, 0, 1, 1, 0, 0, 0] & J_{22} &= j[0, 1, 0, 1, 1, 0, 1, 2, 0, 0, 0] \\
J_{23} &= j[0, 1, 0, 1, 2, 0, 1, 1, 0, 0, 0] & J_{24} &= j[1, 1, 0, 1, 1, 0, 1, 1, 0, 0, 0] \\
J_{25} &= j[0, 1, 1, 1, 1, 0, 1, 1, 0, 0, 0] & J_{26} &= j[0, 1, 2, 1, 1, 0, 1, 1, 0, 0, 0] \\
J_{27} &= j[0, 2, 1, 1, 1, 0, 1, 1, 0, 0, 0] & J_{28} &= j[0, 1, 1, 1, 2, 0, 1, 1, 0, 0, 0] \\
J_{29} &= j[0, 1, 1, 2, 1, 0, 1, 1, 0, 0, 0] & J_{30} &= j[0, 1, 1, 1, 0, 1, 1, 1, 0, 0, 0] \\
J_{31} &= j[1, 1, 0, 0, 1, 1, 1, 1, 0, 0, 0] & &
\end{aligned} \tag{C.6}$$

References

- [1] M. Misiak et al., *Estimate of $\mathcal{B}(B \rightarrow X_s \gamma)$ at $O(\alpha_s^2)$* , Phys. Rev. Lett. 98 (2007) 022002 [arXiv:hep-ph/0609232 [hep-ph]].
- [2] M. Misiak et al., *Updated NNLO QCD predictions for the weak radiative B-meson decays*, Phys. Rev. Lett. 114 (2015) 221801 [arXiv:1503.01789 [hep-ph]].
- [3] M. Misiak, A. Rehman, M. Steinhauser, *Towards $B \rightarrow X_s \gamma$ at the NNLO in QCD without interpolation in m_c* , JHEP 06 (2020) 175 [arXiv:2002.01548 [hep-ph]].
- [4] K. Bieri, C. Greub and M. Steinhauser, *Fermionic NNLL corrections to $b \rightarrow s \gamma$* , Phys. Rev. D **67** (2003), 114019 [arXiv:hep-ph/0302051 [hep-ph]].
- [5] C. Greub, T. Hurth and D. Wyler, *Virtual $O(\alpha_s)$ corrections to the inclusive decay $b \rightarrow s \gamma$* , Phys. Rev. D **54** (1996), 3350-3364 [arXiv:hep-ph/9603404 [hep-ph]].
- [6] G. Buchalla, A. J. Buras and M. E. Lautenbacher, *Weak decays beyond leading logarithms*, Rev. Mod. Phys. **68**, 1125 (1996) [hep-ph/9512380].
- [7] J. Aebischer, M. Fael, C. Greub and J. Virto, *B physics Beyond the Standard Model at One Loop: Complete Renormalization Group Evolution below the Electroweak Scale*, JHEP **1709**, 158 (2017) [arXiv:1704.06639 [hep-ph]].
- [8] J. Klappert, F. Lange, P. Maierhöfer and J. Usovitsch, *Integral reduction with Kira 2.0 and finite field methods*, Comput. Phys. Commun. **266** (2021), 108024 [arXiv:2008.06494 [hep-ph]].
P. Maierhöfer, J. Usovitsch and P. Uwer, *Kira—A Feynman integral reduction program*, Comput. Phys. Commun. **230** (2018), 99-112 [arXiv:1705.05610 [hep-ph]].
R. H. Lewis, *Computer Algebra System Fermat*, <https://home.bway.net/lewis>
- J. Klappert, S. Y. Klein and F. Lange, *Interpolation of dense and sparse rational functions and other improvements in FireFly*, Comput. Phys. Commun. **264** (2021), 107968 [arXiv:2004.01463 [cs.MS]].
- J. Klappert and F. Lange, *Reconstructing rational functions with FireFly*, Comput. Phys. Commun. **247** (2020), 106951 [arXiv:1904.00009 [cs.SC]].
- [9] J. Usovitsch, *Factorization of denominators in integration-by-parts reductions*, [arXiv:2002.08173 [hep-ph]].
- [10] S. Laporta, *High precision calculation of multiloop Feynman integrals by difference equations*, Int. J. Mod. Phys. A **15** (2000), 5087-5159 [arXiv:hep-ph/0102033 [hep-ph]].

- [11] R. N. Lee, *Presenting LiteRed: a tool for the Loop InTEgrals REDuction*, arXiv:1212.2685 [hep-ph].
R. N. Lee, *LiteRed 1.4: a powerful tool for reduction of multiloop integrals*, J. Phys. Conf. Ser. **523** (2014), 012059 [arXiv:1310.1145 [hep-ph]].
- [12] J. M. Henn, *Multiloop integrals in dimensional regularization made simple*, Phys. Rev. Lett. **110**, 251601 (2013) [arXiv:1304.1806 [hep-th]].
- [13] H. M. Asatrian, C. Greub and J. Virto, *Exact NLO matching and analyticity in $b \rightarrow sll$* , JHEP **04** (2020), 012 [arXiv:1912.09099 [hep-ph]].
- [14] A. B. Goncharov, *Multiple polylogarithms, cyclotomy and modular complexes*, Math. Res. Lett. **5**, 497 (1998) [arXiv:1105.2076 [math.AG]].
- [15] H. Frellesvig, D. Tommasini and C. Wever, *On the reduction of generalized polylogarithms to Li_n and $Li_{2,2}$ and on the evaluation thereof*, JHEP **1603**, 189 (2016) [arXiv:1601.02649 [hep-ph]].
- [16] C. Meyer, *Algorithmic transformation of multi-loop master integrals to a canonical basis with CANONICA*, Comput. Phys. Commun. **222**, 295 (2018) [arXiv:1705.06252 [hep-ph]].
- [17] V. A. Smirnov, *Asymptotic expansions in momenta and masses and calculation of Feynman diagrams*, Mod. Phys. Lett. A **10** (1995) 1485 [hep-th/9412063].
- [18] B. A. Kniehl, A. F. Pikelner and O. L. Veretin, *Three-loop massive tadpoles and polylogarithms through weight six*, JHEP **08** (2017), 024 [arXiv:1705.05136 [hep-ph]].
- [19] J. Carter and G. Heinrich, *SecDec: A general program for sector decomposition*, Comput. Phys. Commun. **182**, 1566 (2011) [arXiv:1011.5493 [hep-ph]].
S. Borowka, G. Heinrich, S. P. Jones, M. Kerner, J. Schlenk and T. Zirke, *SecDec-3.0: numerical evaluation of multi-scale integrals beyond one loop*, Comput. Phys. Commun. **196**, 470 (2015) [arXiv:1502.06595 [hep-ph]].
- [20] S. Borowka, G. Heinrich, S. Jahn, S. P. Jones, M. Kerner, J. Schlenk, T. Zirke, *pySecDec: A toolbox for the numerical evaluation of multi-scale integrals*, Comput.Phys.Comm. **222** (2018), [arXiv:1703.09692].
S. Borowka, G. Heinrich, S. Jahn, S. P. Jones, M. Kerner, J. Schlenk, *A GPU compatible quasi-Monte Carlo integrator interfaced to pySecDec*, Comput.Phys.Commun. **240** (2019), [arXiv:1811.11720].
G. Heinrich, S. Jahn, S. P. Jones, M. Kerner, F. Langer, V. Magerya, A. Poldaru, J. Schlenk, E. Villa, *Expansion by regions with pySecDec*, (to appear).

- T. Hahn, *CUBA: A Library for multidimensional numerical integration*, 2005, Comput.Phys.Comm.168, 78-95, [arXiv:hep-ph/0404043].
- T. Hahn, *Concurrent Cuba*, 2016, Comput.Phys.Comm.207, 341-349, [arXiv:1408.6373].
- J. A. M. Vermaseren, *New features of FORM*, arXiv:math-ph/0010025.
- J. Kuipers, T. Ueda, J. A. M. Vermaseren, *Code Optimization in FORM*, 2015, Comput.Phys.Comm.189, 1-19, arXiv:1310.7007.
- M. Galassi, J. Davies, J. Theiler, B. Gough, G. Jungman, P. Alken, M. Booth, F. Rossi, *GNU Scientific Library Reference Manual - Third Edition*, 2009, Network Theory Ltd., ISBN: 0-9546120-7-8 (ISBN-13: 978-0-9546120-7-8), available at <http://www.gnu.org/software/gsl/>
- W. Bruns and B. Ichim and T. Römer and R. Sieg and C. Söger, *Normaliz. Algorithms for rational cones and affine monoids*, available at <https://www.normaliz.uni-osnabrueck.de>
- W. Bruns, B. Ichim, C. Söger, *The power of pyramid decomposition in Normaliz*, 2016, J.Symb.Comp.74, 513–536, [arXiv:1206.1916].
- Z. Li, J. Wang, Q.-S. Yan, X. Zhao, *Efficient Numerical Evaluation of Feynman Integrals*, 2016, Chin.Phys.C40 No. 3, 033103, [arXiv:1508.02512].
- [21] J. Vollinga, *GiNaC: Symbolic computation with C++*, Nucl. Instrum. Meth. A **559** (2006), 282-284 [arXiv:hep-ph/0510057 [hep-ph]].
- [22] <https://ginac.de/tutorial/>
- [23] J. Vollinga and S. Weinzierl, *Numerical evaluation of multiple polylogarithms*, Comput. Phys. Commun. **167** (2005), 177 [arXiv:hep-ph/0410259 [hep-ph]].
- [24] R. N. Lee, *Libra: A package for transformation of differential systems for multiloop integrals*, Comput. Phys. Commun. **267** (2021), 108058 [arXiv:2012.00279 [hep-ph]].
- [25] M. Beneke and V. A. Smirnov, *Asymptotic expansion of Feynman integrals near threshold*, Nucl. Phys. B **522** (1998), 321-344 [arXiv:hep-ph/9711391 [hep-ph]].
- [26] V. A. Smirnov, *Applied asymptotic expansions in momenta and masses*, Springer Tracts Mod. Phys. 177 (2002) 1–262.
- [27] V. A. Smirnov, *Analytic tools for Feynman integrals*, Springer Tracts Mod.Phys. 250 (2012) 1–296.
- [28] A. V. Smirnov, N. D. Shapurov and L. I. Vysotsky, *FIESTA5: Numerical high-performance Feynman integral evaluation*, Comput. Phys. Commun. **277** (2022), 108386 [arXiv:2110.11660 [hep-ph]].

- [29] S. Borowka, G. Heinrich, S. Jahn, S. Jones, M. Kerner, J. Schlenk, *A gpu compatible quasi-monte carlo integrator interfaced to py-secdec*, Computer Physics Communications 240 (2019) 120–137.
- [30] T. Hahn, *Cuba - a library for multidimensional numerical integration*, Computer Physics Communications 168 (2005) 78 - 95.
URL: <http://www.sciencedirect.com/science/article/pii/S0010465505000792>.
- [31] E. Panzer, *Algorithms for the symbolic integration of hyperlogarithms with applications to Feynman integrals*, Comput. Phys. Commun. **188** (2015), 148-166 [arXiv:1403.3385 [hep-th]].